Journal of Applied Phycology
https://doi.org/10.1007/s10811-024-03337-4

RESEARCH

Microfluidic chip-assisted separation process and post-chip microalgae cultivation for carotenoid production

Beyza Karacaoğlu[1,2] · Anıl Tevfik Koçer[1,2] · Benan İnan[1,2] · İsmail Bütün[3,4] · Rabia Mercimek[3,4] · Morteza Ghorbani[3,4,5] · Ali Koşar[3,4,5] · Didem Balkanlı[1,2]

Received: 16 April 2024 / Revised: 5 August 2024 / Accepted: 7 August 2024

Abstract

In many fields of biotechnology, pure microalgae cultures isolated from mixed cultures that exist in nature are needed as raw material sources for the production of high-quality products such as nutraceuticals, cosmetics and biofuels. Regarding the isolation of microalgae, microfluidic systems have gained popularity in recent years due to their low energy and chemical requirements for rapid and effective separation. In this study, optimum flow rates were determined using spiral microfluidics for the separation of microalgae from bacteria, followed by the cultivation of separated microalgae. Then the microalgae obtained in the green phase were subjected to nutrient stress to induce carotenoid production. Carotenoids were extracted after 30-day cultivation, and characterization analyses were performed. Subsequently, the SuperPro Designer® software was used to determine the potential for large-scale carotenoid production from *Chlorella minutissima*. The experiments showed that the fabricated microfluidic system achieved a separation yield and purity of 84.9% and 93.8%, respectively. Furthermore, a 2.5-fold increase in growth rate and carbohydrate and an approximately 1.3-fold increase in protein, lipid, and pigment contents were observed in the post-chip culture. Additionally, a 170% increase in carotenoids was observed within 20 days after induction with nutrient stress. Also, it was shown that microalgal carotenoids could be produced in large scale from *C. minutissima* by recultivating post-chip microalgae and subjecting them to nutrient stress. This study considered multiple flow rates in microchannels designed to separate microalgae from bacteria and carotenoid production from sorted microalgae for the first time.

Keywords *Chlorella* · Microfluidic technology · Inertial microfluidics · Bioprocess · Carotenoids

Introduction

Microalgae are a potential source of natural carotenoids and other important biomolecules, providing an alternative to synthetic molecules that currently dominate the worldwide market (Maltsev et al. 2021; Sousa et al. 2023). Moreover, they have positive environmental impacts, such as maintaining the balance of atmospheric carbon dioxide (Onyeaka et al. 2021) and supporting marine biodiversity (Han et al. 2019a, b, c). Due to these characteristics, extensive research has been conducted on microalgae in recent years. In this regard, obtaining microalgae in pure culture is a fundamental step for both academic research and industrial production (Lee et al. 2020). This step facilitates a better understanding and manipulation of the biological, physiological, and genetic characteristics of microalgae in scientific researches, while in the industry, it enables the control of microalgal growth and biochemical components, thereby ensuring

✉ Didem Balkanlı
didem.balkanli@yildiz.edu.tr

1 Bioengineering Department, Yildiz Technical University, 34220, Esenler, Istanbul, Türkiye

2 Health Biotechnology Joint Research and Application Center of Excellence, 34220, Esenler, Istanbul, Türkiye

3 Faculty of Engineering and Natural Sciences, Sabanci University, 34956, Tuzla, Istanbul, Türkiye

4 Nanotechnology Research and Application Centre (SUNUM), Sabancı University,, 34956, Tuzla, Istanbul, Türkiye

5 EFSUN - Center of Excellence On Nano Diagnostics, Sabanci University, 34956, Tuzla, Istanbul, Türkiye

Published online: 27 August 2024

product quality and stability (Çinar et al. 2018). For these reasons, the processes of microalgae isolation and purification are crucial tasks that need to be thoroughly investigated and optimized with effective and innovative approaches (Fernandez-Valenzuela et al. 2021).

The purification and isolation stage involves the separation and isolation of microalgae from contaminants using physical and chemical methods such as centrifugation, filtration, flocculation, and sedimentation (Singh et al. 2015). During the purification and isolation process, microalgae are rendered axenic using some traditional or advanced isolation techniques based on their cell size, shape, or biochemical properties, and then they are grown under laboratory conditions or in industrial scale depending on the intended applications (Alam et al. 2019). Common methods for microalgae isolation include micropipette isolation, dilution isolation, gravity isolation, phototaxis isolation, and antibiotic isolation (Çinar et al. 2018). Among these, antibiotics are one of the most commonly used methods, as they eliminated unwanted organisms and promote the growth of desired microalgae species; however, controlled use of antibiotics is crucial to mitigate the risk of developing resistant microorganisms (Fernandez-Valenzuela et al. 2021). These challenges have led researchers to explore alternative advanced isolation techniques such as micromanipulation (Singh et al. 2015), flow cytometry (Hyka et al. 2013), and microfluidic chip systems (Karacaoğlu et al. 2023a, b).

Microfluidics provides unprecedented capabilities in the manipulation of small quantities of fluids inside microscale channels (Lin 2011). The separation of microorganisms is an interesting use of microfluidics that is essential in many sectors, including clinical diagnosis, environmental monitoring, and biomedical engineering (Yang et al. 2020). Microfluidic devices are capable of efficiently separating different microorganisms according to their size, shape, deformability, surface charge, and other biophysical characteristics by ingenious designing and modifying microscale structures. These devices use the principles of electrokinetics, hydrodynamics, and surface chemistry to drive the controlled movement of microorganisms which results in very accurate and efficient separation (Bhagat et al. 2010). Furthermore, in comparison to traditional methods, the miniaturization in microfluidic devices enables quick analysis, smaller sample quantities, and higher throughput. Microfluidic platforms hold immense promise in revolutionizing the manipulation and analysis of microorganisms, paving the way for groundbreaking advancements in biotechnology and healthcare. Applications of these platforms range from sorting bacteria for antibiotic susceptibility testing to isolating rare circulating tumor cells for cancer diagnostics (Yan et al. 2017). Regarding the use of microfluidics for separating microorganisms, the separation of microalgae constitutes a particular application (Vu et al. 2018).

Microfluidic devices can efficiently separate microorganisms such as microalgae, enable precise harvesting and processing and overcome challenges in traditional methods thanks to microscale control of particle behavior and fluid flows (Yan et al. 2017). By forming microchannels, traps, and sorting structures that are specifically matched to the dimensions, density, and buoyancy of microalgae cells, microfluidic devices can efficiently separate and concentrate target species from complex culture media while requiring less processing time and energy (Aghakhani et al. 2021). Moreover, real-time adjustment of separation parameters, such as flow rates, applied forces, and channel geometries make it possible thanks to the integration of online monitoring and control capabilities. This allows for the optimization of separation efficiency and purity while limiting energy inputs and waste generation (Huh et al. 2007). The ability to precisely regulate the separation processes improves the economic and scalability of microalgae cultivation. It also makes it easier to carry out subsequent processing steps, including biomass conversion, cell lysis, and lipid extraction, which raises the yield and productivity in a range of applications (Karacaoğlu, et al. 2023a, b). Microfluidic devices are cost-effective methods due to their small size, minimal reagent/chemical requirements, automation capabilities and short experimental times (Veltri & Holland 2020; Bissonnette-Dulude et al. 2023). Although, active-type microfluidic devices that require external forces such as electric or magnetic fields can increase the costs and complexity of experiments (Gou et al. 2018).

Flow rate is a crucial parameter for manipulating cells as it causes shear stress on the cells, which can influence interaction and metabolic responses between cells (Vanapalli et al. 2009; Mu et al. 2013). For instance, the alterations in nanocarrier characteristics such as drug loading capacity, shape and kinetic delivery boundaries, are influenced by variations in microchannel geometry and flow rate which highlights the significance of this parameter (Ahadian et al. 2020; Lingadahalli Kotreshappa et al. 2023). The related study demonstrated that microalgae re-cultured after the microfluidic stream exhibited more effective growth compared to single microalgae cells (Wu et al. 2023). In this context, microfluidic devices can be utilized to induce the production and extraction of carotenoids like astaxanthin (Kwak et al. 2015; Cheng et al. 2018; Yao et al. 2020) or lipids (Bensalem et al. 2018; Han et al. 2019a, b, c; Mishra et al. 2021). The progress in microalgae cultivation and selection techniques has led to new opportunities for utilizing microalgae in the industry including pharmaceuticals, nutrition, and biofuels (Kim et al. 2018; Ozdalgic et al. 2021).

Motivated by the abovementioned advantages of microfluidic devices, the purpose of this study is to separate microalgae from bacteria with a high separation efficiency and to examine, evaluate, and analyze the effect of microfluidic

channels on microalgae. This study employs microfluidic platforms that leverage advancements in microalgae separation via inertial microfluidics. Although there are studies on the separation of microalgae with microfluidic chips in the literature, there is limited literature on the optimization of separation processes and observation of the effect of using microfluidic systems with spiral channels on microalgae growth. This research fills the gap in the literature on the use of microfluidic systems for the separation of microalgae from bacteria, optimization studies, the effect of flow rate on microalgae cultivation, and the use of post-chip microalgae in further studies. This study considered multiple flow rates in spiral microchannels specifically designed to separate microalgae and bacteria and employed the separated microalgae for carotenoid production for the first time.

Materials and methods

Chlorella minutissima and *Escherichia coli* ATCC 25922 were used. The experiments were conducted at Yildiz Technical University Algal Biotechnology and Bioprocess Laboratory and Sabanci University Nanotechnology Research and Application Center (SUNUM). The experimental steps are summarized in Fig. 1.

Preparation of the microorganisms

The process incorporates the use of *C. minutissima* microalgae and *E. coli* bacteria to separate these two different kinds of microorganisms and to acquire concentrated microalgae. *Chlorella minutissima*, supplied from the Culture Collection of Algae at Göttingen University (Germany) and the Algal Biotechnology and Bioprocess Laboratory of Yildiz Technical University (Türkiye), was cultivated in 250-mL Erlenmeyer flasks using BG-11 nutrient medium (İnan et al. 2023). The cultivation took place in a shaking incubator for a duration of 14 days under a temperature of 25 °C, a light intensity of 100 µmol photons m^{-2} s^{-1} continuous illumination, pH 7.2, and a shaking speed of 150 rpm (Koçer et al. 2021).

Eschericia coli ATCC 25922 was incubated in a sterile glass bottle with nutrient broth (Merck, Germany) for 10 mL of working volume at 37 °C for 24 h in an incubator. The absorbance values of the microalgae and bacteria cultures were quantified at 680 nm and 600 nm, respectively. A Neubauer slide was used for counting microalgae whereas the McFarland technique was utilized for counting bacteria cells. A bacterial cell count of 0.5 McFarland units was determined. The concentration of *C. minutissima* in the mixture was adjusted to be 10 times the concentration of *E. coli* (Higgins & VanderGheynst 2014) that consists of distilled water to standardize the microfluidic separation process experiment.

Eschericia coli was chosen as the bacterium for this experiment because of its well-understood genetics and fermentation technology, easy and rapid culturability, and it is one of the most common bacterial contaminants in many microalgal cultures. Therefore, it was considered a suitable model for comparing and interpreting results with other studies related to microfluidic systems and having more reliable results (Germond et al. 2013; Higgins & VanderGheynst 2014).

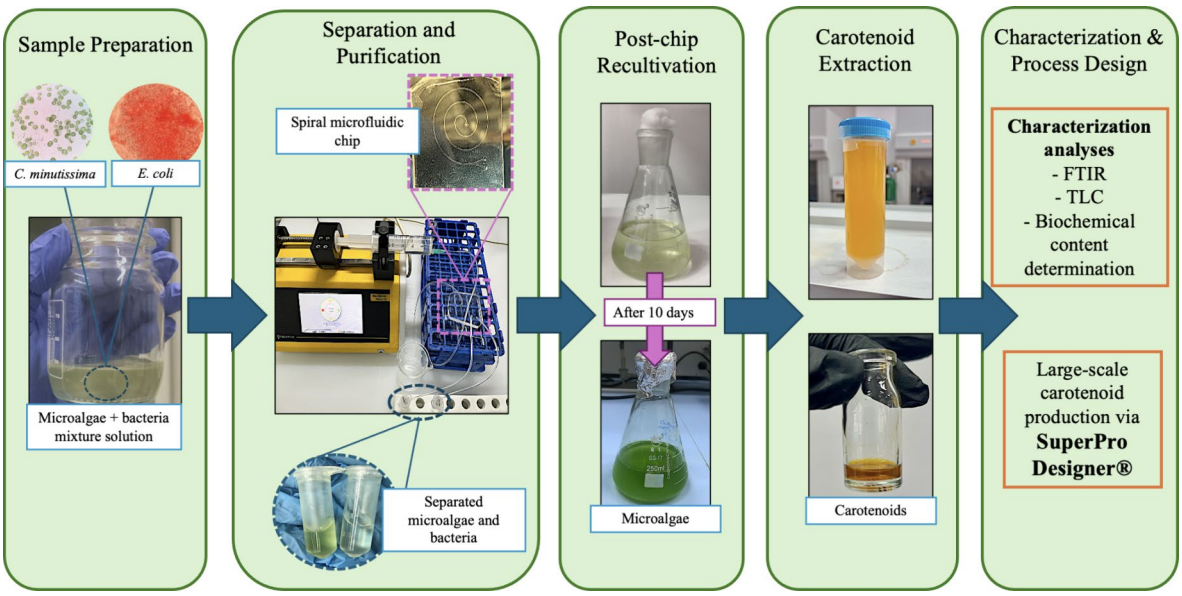

Fig. 1 Experimental set-up for carotene production from *Chlorella minutissima*

Theory

Due to the dominance of viscosity over inertial forces in microfluidic systems, the flow in microchannels is primarily laminar, with a Reynolds number (Re) < 2300 (Bragheri et al. 2020; Otzen et al. 2021). To separate particles or cells of various sizes in spiral microchannels, the balance between two distinct forces is employed inside the fluid flow: inertial lift forces (F_L) and Dean drag forces (F_D). F_L consist of shear gradient-induced forces, which are dependent on flow velocity, and wall-induced buoyancy forces, which arise from the interaction of the flow with a surface (Erdem et al. 2020; Wang et al. 2020):

$$F_L = \frac{f_L q_f {U_{max}}^2 {a_p}^4}{{D_h}^2} \tag{1}$$

$$D_h(m) = \frac{2hw}{h+w} \tag{2}$$

where f_L is the lift coefficient, q_f is the fluid density, α is the particle diameter, U_{max} is the maximum flow velocity, and D_h is the hydraulic diameter. A spiral microchannel has a rectangular cross-section while w is the width and h is the height of the microchannel.

In spiral microchannels centrifugal effects cause a secondary flow from the inner wall to the outer wall. This secondary flow appears to play a significant role in separating particles. The formation of two Dean vortices occurs in spiral microchannels due to the presence of this secondary flow (Syed et al. 2018; Kim et al. 2021). Due to the Dean vortices created by the Dean drag effect, particles of varying sizes migrate towards the inner or outer regions of the microchannels, leading to the separation of particles based on the size within microchannels (Lee & Yao 2018; Mihandoust et al. 2020; Karacaoğlu 2024):

$$F_D = 3\pi\mu U_{De} a_p \tag{3}$$

where μ is the fluid dynamic viscosity and U_{De} is the Dean velocity. Dean velocity is expressed as:

$$U_{De} = 1.8{\times}10^{-4}{\times}De^{1.63} \tag{4}$$

where De is the dimensionless Dean number and is calculated as:

$$De = \frac{q_f U_f D_h}{\mu} \times \sqrt{\frac{D_h}{2R}} = Re \times \sqrt{\frac{D_h}{2R}} \tag{5}$$

$$Re = \frac{q_f U_f D_h}{\mu} \tag{6}$$

$$U_f(m/s) = \frac{Q}{A} \tag{7}$$

where U_f is the average fluid velocity, R is the radius of curvature, Re is the dimensionless Reynolds number, Q is flow rate and A is the cross-sectional area (Özbey et al. 2019; Altay et al. 2022). The particle size has a significant impact on the inertial lift forces and Dean drag forces.

The liquid density (1030 kg m^{-3}) and the viscosity of the liquid (0.0008 kg ms^{-1}) were used according to the microalgae culture medium in the calculations (Barten et al. 2022) while the average value of lift coefficient is 0.5 in practice (Lee & Yao 2018; Wang et al. 2020).

Design and microfabrication of the spiral microfluidic device

The spiral microfluidic chip design was created using the AUTOCAD software (2018) with the aim of separating microalgae from bacteria of different dimensions and collecting concentrated microalgae. The design parameters for the 2D spiral microchannel were determined in the light of previous study (Erdem et al. 2020) as: 5 turns, channel height of 100 µm, channel width of 500 µm, inner diameter of the entrance channel of 2 cm, and radius of curvature of 5 mm. Furthermore, the microfluidic device incorporates an input channel to facilitate the transfer of a mixed culture, as well as two distinct outlet channels to effectively separate cells based on their different sizes (Mihandoust et al. 2020). The standard soft lithography technique was utilized to fabricate the polydimethylsiloxane (PDMS) spiral microchannel (Erdem et al. 2020). All microfabrication steps were performed under clean-room conditions at the Sabancı University Nanotechnology Research and Application Center (SUNUM). The parameters for this spiral microfluidic system are displayed in Fig. 2. The particle sizes of 1.5 µm and 6 µm were utilized in this context due to the ImageJ image processing results indicating that the average size of *C. minutissima* was around 6 µm and the average size of *E. coli* was around 1.5 µm (Karacaoğlu 2024).

Experimental set-up and evaluation of microfluidic separation performance

Microalgae were separated from bacteria using the microfluidic platform developed by the soft-lithography technique. Tubings (LMT-55, IDEX Corp., USA) were utilized in microfluidic platforms to provide mixed culture into the input channels as well as to collect samples from the outlet channels. Fittings (IDEX Corp.) were employed to join these pipes to the microfluidic device. The tubing in the input channel was immediately linked to the syringe pump (Inovenso, Nanospinner Starter Kit). The microchannels

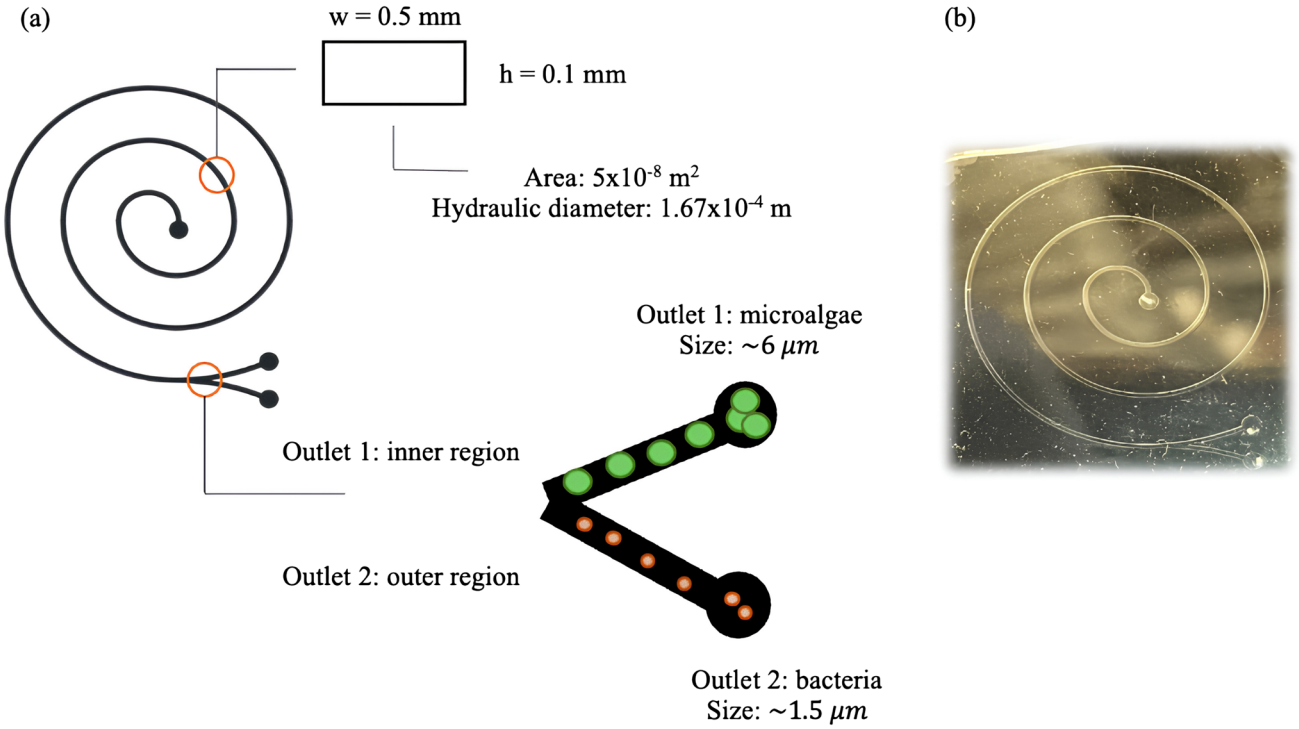

Fig. 2 (**a**) The design parameters of spiral microfluidic system and demonstration of inertial microfluidic separation (**b**) The fabricated PDMS microfluidic device

were cleaned and kept free of contamination by passing 70% ethanol and sterile distilled water through them. Thereafter, the syringe contained a mixed culture that was injected into the microfluidic system using a syringe pump at flow rates ranging from 250 to 3000 µL min^{-1}. All the separation processes with microfluidic chip experiments were performed in triplicate. The impact of flow rate on the separation performance was then evaluated. Following the separation procedure, the samples from the outlet channels were gathered in sterile Eppendorf tubes, and then the microalgae and bacteria in the outlet channels were quantified. The Neubauer slide counting method was utilized for microalgae counting and evaluating the microalgae cell viability in a light microscope (Olympus CX22 microscope), whereas the plate count method was employed for bacterial enumeration. Following the counting of microalgae and bacteria, the best separation performance of the microfluidic platform was assessed using separation yield and purity data (Eq. 8 and 9):

$$\text{Separation Yield } (\%) = \frac{C.minutissima_{outlet,1}}{C.minutissima_{outlet,1\&2} + E.coli_{outlet,1\&2}} \times 100 \quad (8)$$

$$\text{Separation Purity } (\%) = \frac{C.minutissima_{outlet,1}}{C.minutissima_{outlet,1} + E.coli_{outlet,1}} \times 100 \quad (9)$$

All experiments were performed in a microbiological safety cabinet with laminar airflow at the Algal Biotechnology and Bioprocess Laboratory of Yildiz Technical University (Türkiye). Microalgae and bacteria in spiral microchannels experience distinct inertial buoyancy forces and dean drag forces. As a result they focus on different equilibrium positions because of their different sizes. Particle size and flow rate parameters have an impact on the magnitudes of the F_L and F_D. The bacteria move along the secondary flow in the spiral channels towards the outer wall of the microchannels. However, the weak reverse Dean vortices prevent them from being dragged back towards the inner wall which results in the position of microalgae closer to the microchannel inner wall and the position of bacteria near the outer wall, as illustrated in Fig. 2. Additionally, F_L on particles near the microchannel wall increases with Reynolds numbers. Therefore, the flow rate is an important parameter in separating microalgae from bacteria (Martel & Toner 2014; Li et al. 2017; Syed et al. 2018; Huang et al. 2020).

Recultivation of microalgae and biochemical analysis

Following the separation process at the optimum flow rate, the microalgae obtained from outlet channel were cultivated again in BG-11 nutrient medium in a 250-mL Erlenmeyer flask with a working volume of 150 mL for a duration of 10 days. The culture was maintained at a constant temperature of 25 °C under continuous illumination of 100 µmol

photons m^{-2} s^{-1}, pH kept was constant at 7.2 using HCl or NaOH, and a shaking speed of 150 rpm. Simultaneously, *C. minutissima* were cultivated in BG-11 nutrient medium with a working volume of 100 mL for 10 days without passing them through the microfluidic chip as a control. All the recultivation experiments were performed in triplicate. The growth curves of the cultures were determined during cultivation using a UV–Vis spectrophotometer at 680 nm. At the end of the cultivation, the growth kinetics and biochemical contents of the microalgae were examined and compared. The specific growth rate (μ) and doubling time (t_d) were calculated as (Singh et al. 2020):

$$\text{Specific growth rate}\left(\frac{1}{\text{day}}\right) = \frac{\ln(X_2) - \ln(X_1)}{t_2 - t_1} \tag{10}$$

$$\text{Doubling time (day)} = \frac{ln2}{\mu} \tag{11}$$

A comprehensive biochemical content analysis of carbohydrate (DuBois et al. 1956), protein (Lowry et al. 1951), lipid (Bligh & Dyer 1959), and pigment content (Zou & Richmond 2000; Macías-Sánchez et al. 2005) in both post-chip microalgae and pure microalgae culture samples was conducted.

Carotene production and carotene extraction

The microalgae collected after the microfluidic chip and maintained in a viable state, were re-suspended and cultured in BG-11 medium within a 250-mL flask, with a working volume of 100 mL. The culture was incubated at a stable temperature of 25 °C with constant illumination of 100 μmol photons m^{-2} s^{-1}, pH 7.2, and 150 rpm stirring. There was no nutrient addition to the culture medium during the 30-day cultivation period to facilitate the microalgal transition from the green phase to the red phase (Minyuk et al. 2020). This transition was crucial for optimal pigment production and biomass accumulation in microalgal cultivation. After 30 days, 50 mL of microalgae culture was centrifuged at 8000 rpm for 10 min, washed twice with distilled water, and dried in an oven at 60 °C for 24 h and stored for further analysis and extraction of carotenoids (Ratha et al. 2016). The remaining culture was stored at 4 °C for biochemical content analysis.

For carotenoid extraction a 1:1 mixture of hexane and acetone was used (Mariana et al. 2016). Briefly, 0.2 g of dried microalgae was dissolved in 3.5 mL of total solvent (Rusdianasari et al. 2021) and the mixture incubated at 50 °C in a water bath for 3 h with continuous shaking (Rajput et al. 2022). The extract was filtered with 0.45 μm filters once the separation was complete to remove any remaining biomass particles before characterization analysis. All the carotene production experiments were performed in triplicate.

Characterization analyses

After the 30 days cultivation period, the stored microalgae culture was analyzed for the total carbohydrate (DuBois et al. 1956), protein (Lowry et al. 1951), lipid (Bligh & Dyer 1959), and pigment content.

The functional groups present in the dried microalgae sample and nearly 2 mg of a β-carotene analytical standard (Sigma-Aldrich, 99%) were examined using Fourier-transform infrared spectroscopy (FTIR) analysis with a Bruker Alpha FT-IR instrument. The dry biomass was placed directly onto the attenuated total reflectance (ATR) crystal for obtaining the sample spectrum within a wavenumber range of 4000 cm^{-1} to 500 cm^{-1}, with a resolution of 4 cm^{-1} and 32 scans (Koçer et al. 2020; Quijano-Ortega et al. 2020).

The pigment content was determined by microalgal extract from green microalgae with optical density measurements at 666 nm and 475 nm using a UV–Vis spectrophotometer, and the chlorophyll-*a* and total carotenoid content were calculated from Eq. 12–13 (Zou & Richmond 2000; Macías-Sánchez et al. 2005):

$$\text{Chlorophyll} - a\ (\mu\text{g mL}^{-1}) = 13.9 \times OD_{666} \tag{12}$$

$$\text{Carotenoid}\ (\mu\text{g mL}^{-1}) = 4.5 \times OD_{475} \tag{13}$$

TLC was used to separate and identify the various carotenoids present in the microalgal extract. Microalgal extract was (10 μL) spotted onto a 15-cm TLC silica gel plate (TLC silica gel 60 F254, Merck) as stationary phase using microcaps, along with a standard of β-carotene. The sample-loaded TLC plate was developed in a chamber using a solvent mix of hexane and acetone in a 75:25 (v/v) ratio as mobile phase (Bhagavathy et al. 2011; Joseph et al. 2022). After development, the TLC plate was visualized to detect the presence of β-carotene and other carotenoids as spots of different location and color. The retention factor (R_f) values of the compounds were calculated (Pérez et al. 2021; Rajput et al. 2022).

Modeling and simulation approach for carotenoid production using software

SuperPro Designer® software v8.0. (Intelligen, Inc., USA) was used to assess the feasibility of large-scale production of carotenoids and to design and simulate this process from *C. minutissima*. The software has numerous unit procedures for designing carotenoid production and enabled extensive analysis of numerous production factors and identified possible weaknesses in the process. This complete approach allowed for the

optimum process strategy regarding the efficiency and yield. The design of the process comprised three basic steps: the cultivation strategy (green and red phases) was implemented, biomass was recovered, and carotenoids were separated.

Results

Force calculations and design of microfluidic platform

Table 1 presents the Reynolds and Dean numbers, Dean velocity and Dean drag and inertial lift forces which were obtained in the light of the section Theory, for microalgae and bacteria according to each flow rate. They serve in examining the behavior of flow and particles in microfluidic device.

Separation performance of the microfluidic platform

Figure 3 illustrates the performance of the microfluidic platform featuring 5-turns spiral microchannels, focusing on the separation efficiency and separation purity at various flow rates. The inlet flow rate ranged from 250 to 3000 L min^{-1}, corresponding to Reynolds numbers ranging from 18.3 to 219.4.

The results revealed that the microalgae cells migrated to one side of the channel and concentrated at an equilibrium position. In the microfluidic platform featuring 5-turns spiral microchannels, the high separation efficiencies were at 36.6, 73.1 and 109.7 Reynolds numbers, yielding efficiencies of 84.3%, 83.6%, and 82.1%, respectively. Conversely, at 18.3, 146.3, 182.9 and 219.4 Reynolds numbers, separation efficiencies remain below 80%. Notably, the lowest separation

Table 1 Fluid mechanics-related calculations

				Microalgae		Bacteria	
Flow rate (μL min^{-1})	Reynolds number	Dean number	Dean velocity	Dean Drag Force (N)	Inertial Lift Force (N)	Dean Drag Force (N)	Inertial Lift Force (N)
250	18.3	0.11	4.68×10^{-6}	2.11×10^{-13}	1.67×10^{-13}	5.28×10^{-14}	6.52×10^{-16}
500	36.6	0.21	1.45×10^{-5}	6.54×10^{-13}	6.67×10^{-13}	1.63×10^{-13}	2.61×10^{-15}
1000	73.1	0.43	4.49×10^{-5}	2.02×10^{-12}	2.67×10^{-12}	5.06×10^{-13}	1.04×10^{-14}
1500	109.7	0.64	8.69×10^{-5}	3.92×10^{-12}	6.01×10^{-12}	9.8×10^{-13}	2.35×10^{-14}
2000	146.3	0.85	1.4×10^{-4}	6.26×10^{-12}	1.07×10^{-11}	1.57×10^{-12}	4.17×10^{-14}
2500	182.9	1.07	2×10^{-4}	9.01×10^{-12}	1.67×10^{-11}	2.25×10^{-12}	6.52×10^{-14}
3000	219.4	1.28	2.7×10^{-4}	1.21×10^{-11}	2.4×10^{-11}	3.04×10^{-12}	9.39×10^{-14}

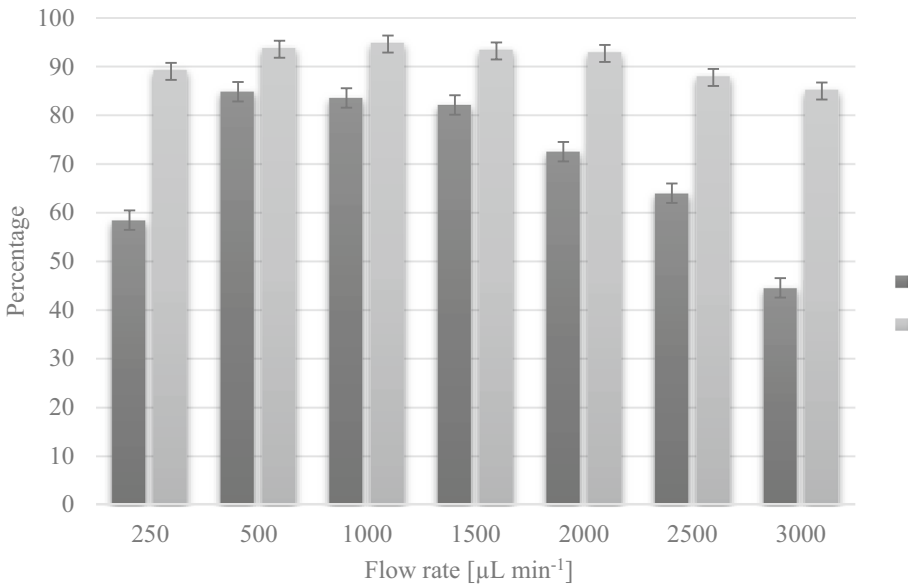

Fig. 3 Separation performance of the microfluidic platform at different flow rates. Average value, ± SD from three independent replicates. Dark bars = Separation yield, light bars – separation purity

efficiency was recorded at 219.4 Reynolds number, with a value of 44.5%. Regarding the separation purity, all results exceeded 85%. The high separation purities were attained at 73.1, 36.6 and 109.7 Reynolds numbers, with values of 94.9%, 93.8%, and 93.5%, respectively. Contrarily, at 219.4 Reynolds number, a purity of 85.3% was achieved. From these results, it can be observed that microalgae culture can be highly purified from bacteria at Reynolds numbers of 36.6, 73.1 and 109.7, and microalgae can be efficiently collected as concentrated form from outlet channel 1 with increased focusing performance of the microfluidic platform. At other Reynolds numbers, although the purification rate remains high, microalgae cannot be collected in concentrated form from outlet channel 1, and a significant number of microalgae is also detected in outlet 2 (Karacaoğlu et al. 2023).

Growth kinetics and biochemical content analysis of post-chip cultivated microalgae

Figure 4 depicts the growth curves of the microalgae cultures. Higher absorbance values and greater biomass were achieved from microalgae passed through the chip under the same conditions and time. For the untreated microalgae culture, the logarithmic (log) phase was determined to be between days 6–10, whereas the log phase for the post-chip microalgae culture was between days 2–6. The calculated μ value for the untreated microalgae culture was 0.133 day^{-1} and t_d was 5.2 days, while for the post-chip microalgae culture, the μ value was 0.34 $day^{-1}$and t_d as 2 days. It was observed that the adaptation (lag) phase of the untreated microalgae culture lasted approximately 5 days, while the lag phase of the post-chip microalgae culture lasted 2 days, which suggest that the post-chip microalgae culture adapted more quickly to the nutrient medium and transitioned rapidly to the log phase.

In Table 2, calculated μ and t_d values are presented along with the biochemical content results of untreated and post-chip microalgae cultures. According to the results of simultaneous analysis, an increase in total carbohydrate, protein, lipid, and pigment content was observed in microalgae passed through the chip. While the total carbohydrate and protein content showed approximately twofold and 1.5-fold increases, respectively, the total chlorophyll increased by 1.4-fold and total lipid and carotenoid by 1.23-fold. The microalgae, once separated from bacteria and re-cultured for a duration of 10 days, exhibited significant and sustained development without any noticeable indications of damage to cells.

Characterization analyses for carotenoid production

Biochemical content analyses

Table 2 displays the biochemical contents of the microalgae culture initiated for carotenoid production after 30 days. There was an approximate 39% decrease in total carbohydrate content compared to the biochemical content results obtained after 10 days of post-chip cultured microalgae (Table 2). Conversely, an increase is observed in total protein, lipid, chlorophyll, and carotenoid contents. The protein and lipid content has increased by approximately 7% and 20%, respectively, while chlorophyll and carotenoid contents have increased by approximately 190% and 170%, respectively.

The highest carbohydrate content and growth rate were achieved in the post-chip microalgae culture at 10 days, while the highest protein, lipid and pigment content were

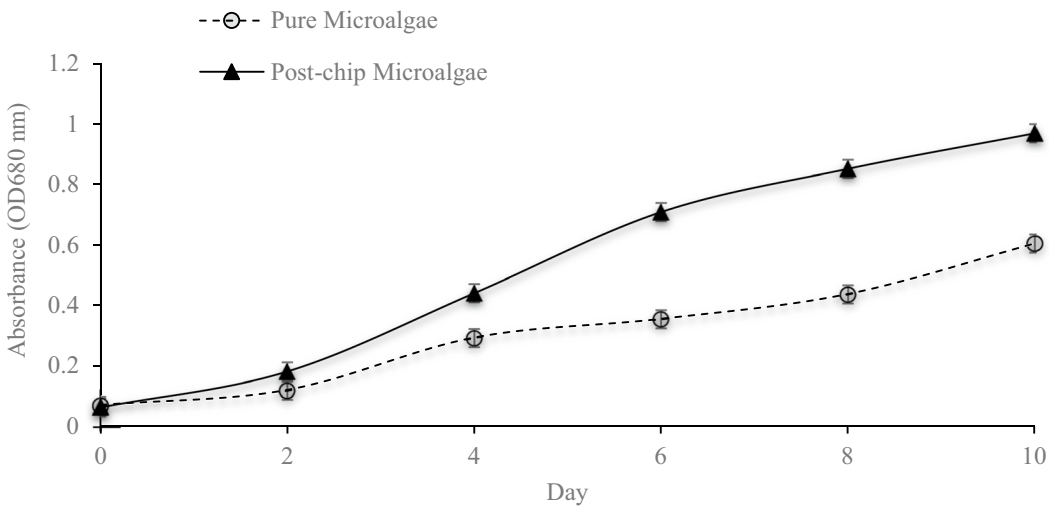

Fig. 4 Growth kinetics of microalgae cultures. Average values ± SD from three independent replicates

Table 2 Biochemical content analysis for microalgae cultures. Data shown are means ± SD from three independent replicates

Biochemical Contents and growth kinetics	Untreated Microalgae Culture 10 days	Post-Chip Microalgae Culture 10 days	Microalgae Culture for Carotene Production 30 days
Specific growth rate (day^{-1})	0.13 ± 0.15	0.34 ± 0.15	0.30 ± 0.2
Doubling time (day)	5.2 ± 0.15	2 ± 0.15	2.28 ± 0.2
Carbohydrate content (μg mL^{-1})	200.5 ± 0.3	400 ± 0.3	243.5 ± 0.2
Protein content (μg mL^{-1})	98.6 ± 0.45	142.86 ± 0.35	152.9 ± 0.3
Lipid content (mg g^{-1})	36.8 ± 0.15	44.4 ± 0.5	55.2 ± 0.2
Chlorophyll content (μg mL^{-1})	2.15 ± 0.2	3 ± 0.2	8.7 ± 0.15
Carotene content (μg mL^{-1})	0.9 ± 0.2	1.11 ± 0.2	3 ± 0.15

obtained in the 30-day nutrient-stressed microalgae culture. These results stem from microalgae producing biomass and primary metabolites such as carbohydrates and proteins under optimal conditions, and secondary metabolites such as chlorophyll and carotenoids under stress conditions (Tong et al. 2023). The decrease in protein and increase in carbohydrates under stress may likely be attributed to the production of certain proteins and amino acids under stress conditions (Kolackova et al. 2023). In the pure microalgae culture not passed through the microfluidic system, the lower values were observed in all parameters. The results show that carotene production can be induced under nutrient stress in microalgae culture.

Fourier-transform infrared spectroscopy

The harvested and dried microalgal biomass at the end of carotenoid production and the β-carotene standard were subjected to FTIR analysis. As can be seen in Fig. 5, there is an overlap between the FTIR spectra of dried biomass of microalgae harvested for carotene production and the β-carotene standard.

β-carotene structure consists of two non-substituted β-ionone rings (Paparella et al. 2021), methyl and alkene groups (Woggon 2002). Although most peaks in the spectrum matched the reference spectrum of β-carotene, the carotenoid extract obtained from *C. minutissima* contains not only β-carotene but also other carotenoid groups. Therefore, more peaks were observed in the spectrum of the microalgal biomass. When the FTIR spectra of the biomass extracted from *C. minutissima* and the β-carotene standard were examined, several peaks were observed. The peaks at 3403.36 and 3355.31 cm^{-1}, for β-carotene and biomass, respectively, correspond to the vibrations of the – OH groups, which are caused by the presence of moisture in the component (Quijano-Ortega et al. 2020). The peak around 1740 cm^{-1} in biomass represents the ester carbonyl functional group of triglycerides (Takeungwongtrakul et al. 2015). In addition, peaks at 1160 and 1240 cm^{-1} in the microalgae biomass spectrum indicate the presence of C = O ester group in triglycerides and fatty acids (Pérez et al. 2021) and peaks in the range of 1650 cm^{-1} corresponds to carbonyl group of aldehydes (Zaid et al. 2015). The peaks seen in the 1710 cm^{-1} range in both microalgal biomass and β-carotene

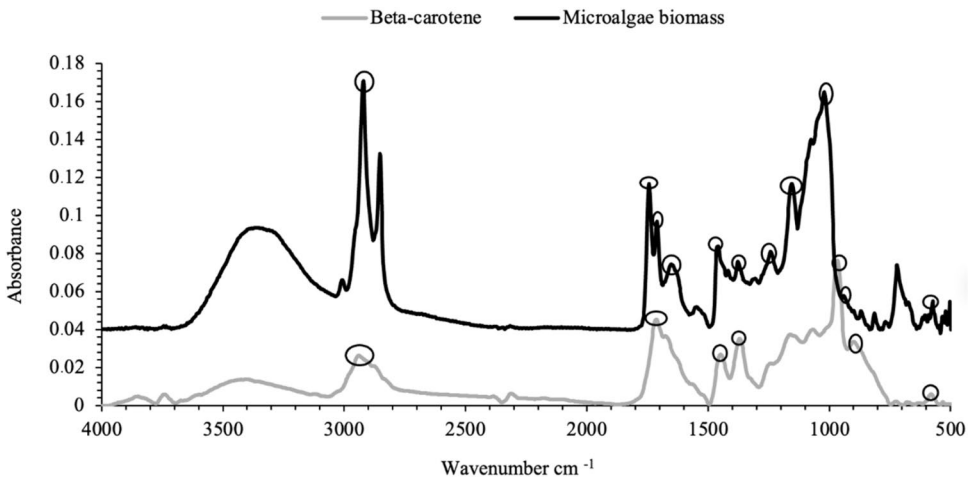

Fig. 5 FTIR analysis for microalgae biomass and the β-carotene standard. Circles in the figure are presented to highlight certain peaks in the FTIR spectrum

spectra represent the alkene group (Lambert 1987). The peaks observed at approximately 1450 cm^{-1} in biomass and β-carotene correspond to the bending and vibration of methylene groups, which could be attributed to lycopene pigments (Neha et al. 2017), whereas the peaks at 1370 cm^{-1} are indicative of umbrella vibrations originating from the CH_3 groups (Elumalai et al. 2014). The highest intensity peak in the β-carotene standard occurs at roughly 970 cm^{-1}, which corresponds to the vibrations caused by the bending of the C-H bonds in the polyene chain. On the other hand, the peak at around 570 cm^{-1} indicates the alterations in the angles and deformations of the polyene chain. The peak at 1020 cm^{-1} in the microalgae biomass, although slightly shifted, is similar to the peak around 570 cm^{-1}. The peaks around 900 cm^{-1} and 2900 cm^{-1} in both spectra appear due to β-ionone rings in the structure of β-carotene (Jalilian 2008). Within microalgae biomass spectra, a specific band may be observed at around 1100 cm^{-1}. This absorbance peak is attributed to the C–O stretch vibrations of alcohols and is likely associated with other carotenoids (Quijano-Ortega et al. 2020).

Thin-layer chromatography

TLC separation exhibited spots in six different locations and colors at R_f values of 0.05, 0.52, 0.64, 0.67, 0.84 and 0.99, respectively (Table 3). The R_f value for the β-carotene and standard was 0.98, which corresponded to the retention time of the carotene extract as shown in Fig. 6. Band 1 in the carotene extract is believed to be connected to phenolic compounds, band 2 to astaxanthin, bands 3 and 4 represent carotenoid isomers, band 5 to α-carotene, and band 6 to β-carotene.

FTIR analysis revealed that the carotenoid extract obtained from the green microalga species *C. minutissima* is structurally similar to β-carotene. However, the presence of other carotenoids in the extract was also evidenced due to some structural differences such as ester or hydroxyl groups in the microalgal biomass. These findings were supported by TLC, where six different colored bands were observed. The presence of β-carotene in the extract was confirmed by TLC development using the same procedure as for the β-carotene standard. In a study conducted with *Ulva lactuca* algae, bands were observed at R_f values of 0.81 and 0.94 in TLC using the same mobile phase as our study (75:25 v/v hexane:acetone), and they were respectively matched with α-carotene and β-carotene (Adb el Baky et al. 2008). Additionally, in another experiment conducted with the same mobile phase, it was observed that phenolic compounds did not migrate on the silica gel plate and remained stationary (de Laguna et al. 2015). Some *Chlorella* species have been reported to be keto-carotenoid producers like astaxanthin (Gong & Huang 2020) and the capacity to produce astaxanthin has been reported in the *C. minutissima* (Ljubic et al. 2021). In the investigation conducted, it was shown that in the hexane:acetone (3:1) mobile phase, astaxanthin monoesters typically yield an R_f value of 0.5 (Dalei and Sahoo 2015) which also clarifies the ester bonds in the FTIR results of microalgae biomass.

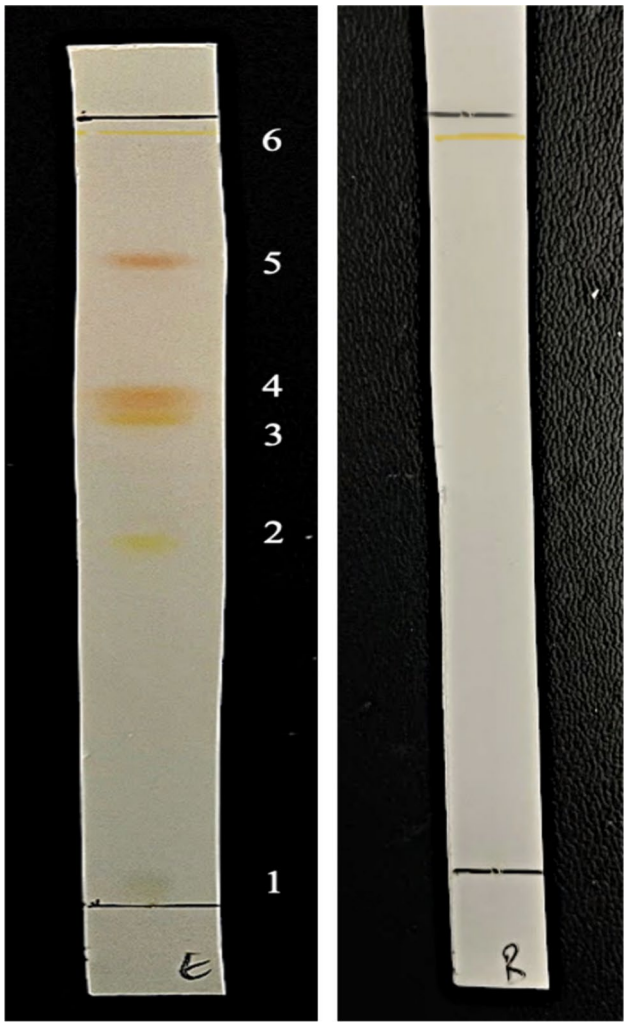

Fig. 6 TLC analysis for carotene extract and β-carotene standard

Table 3 Bands and characteristics in carotenoid extract as observed in TLC analysis

No	R_f Values	Color of Spot	Declared Compound
1	0.05	Green	Phenolic compounds
2	0.52	Yellow	Astaxanthin
3	0.64	Orange	Other carotenoids
4	0.67	Orange	Other carotenoids
5	0.84	Red	α-carotene
6	0.99	Yellow	β-carotene

Process design and simulation

In this section, a large-scale carotene production from *C. minutissima* was designed and the process was carried out via the SuperPro Designer® software. The data from the experimental section was used to develop this process, which consist of two step cultivation by changing the growth media to produce microalgae. Data from the process design and simulation are anticipated to make it easier to determine the productivity, capital, and operating cost thresholds in order to target sale amounts of microalgae (Koçer et al. 2023). Photobioreactor was preferred to ensure efficient production by providing parameter and contamination control to obtain specific products such as carotene, pigment, and other bioactive compounds.

In this process design, microalgae production is operated for 270 days per year. Three months duration in winter season was not appropriate for microalgae cultivation and used for maintenance requirements. The design of the carotene production from microalgae was shown in Fig. 7. In the beginning, *C. minutissima* were first cultivated in 5000 L fermenter (SFR-101) to be used as inoculum by providing nitrate, sulfate, water and carbon dioxide to the fermenter. Then the inoculum was sent to the main fermenter (FR-101) with a working volume of approximately 90.000 L. In order to enter the red phase, nitrate and sulfate amounts that were sent to FR-101 were reduced by half. In these fermenters, reactions were assumed to be carried out with 90% conversion. At the end of the microalgae cultivation, carotene enriched microalgal culture were sent to clarification (CL-101) for dewatering by using flocculant. In this process, 99% of the microalgal biomass was clarified and clarified water was sent to the FR-101 to utilize the water remained after flocculation again. Microalgal sludge was sent to centrifugation (DC-101) and again 99% of the microalgal biomass was centrifuged and freeze dried in FDR-101 to obtain dry microalgal biomass. In FDR-101, 85% of carbon dioxide, oxygen and water evaporated according to the calculations carried out by the software based on final loss on drying. Dry biomass was then sent to homogenization (HG-101) and extraction (SMSX-101) to obtain carotene extract. In this process, total solute recovery yield in liquid phase was adjusted as 95%. To separate volatile solvents and enriched the carotene content, the product was sent to evaporation (EV-101). Here solvents that were used in the extraction step, acetone and hexane were evaporated up to 90%. Finally, the product sent to spray drying (SDR-101) where the 95% of acetone and hexane were removed according to the calculations carried out by the software based on final loss on drying. At the end of the process, product was sent to tableting (TB-101) where 3800 entities/batch were achieved for 90.000 L cultivation. Overall component balance is given in Table 4.

Discussion

Effects of the flow rate on different particle sizes for separation performance

Spiral microchannels can be utilized for the purification of microalgae from contamination or for isolation studies related to natural sources such as oceans, lakes, glaciers, etc. Changes in flow rate can directly affect separation efficiency and purity in inertial microfluidic systems, as channel length, total flow rate, and sheath-to-sample flow rate

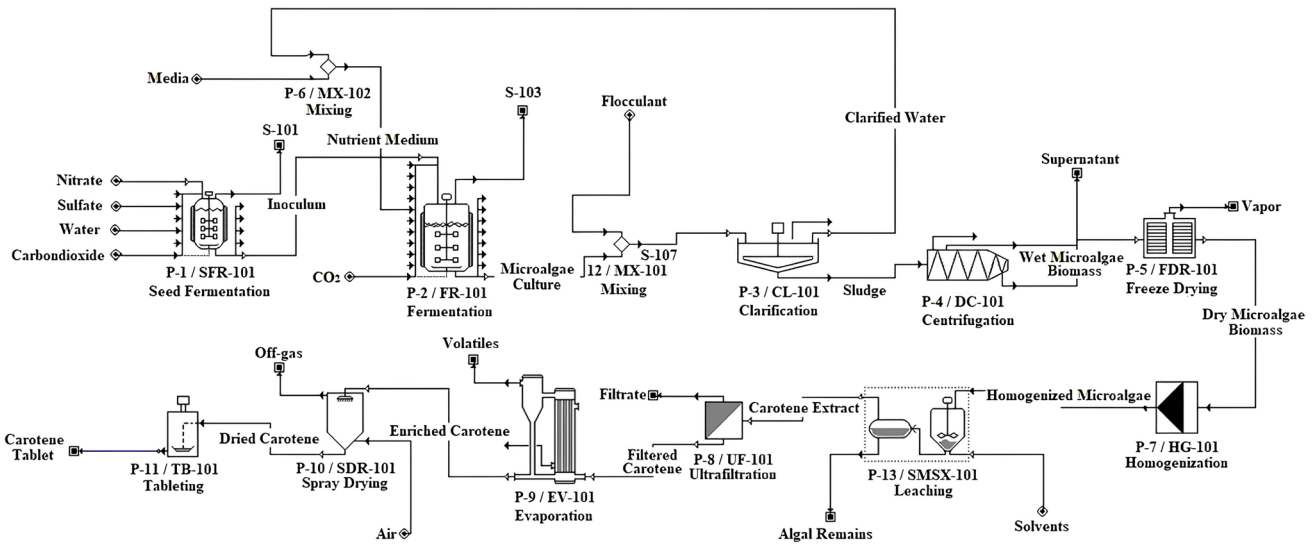

Fig. 7 Base case scenario: Process flow diagram for carotene production from *C. minutissima* using SuperPro Designer®

Table 4 Overall component balance (t year^{-1}) of the designed process

COMPONENT	INITIAL	INPUT	OUTPUT	FINAL	IN–OUT
Acetone	0	35.77	35.77	0	0
Ash	0	0	0.84	0	-0.84
Biomass	0	0	1.06	15.45	-16.52
Carbon dioxide	0	55	5.11	0.39	49.5
Cell debris	0	0	5.13	0	-5.13
Flocculant	0	0.12	0.11	0.01	0
Hexane	0	35.77	35.77	0	0
$NaNO_3$	0	38,623.35	1,103.22	37,507.91	12.22
Nitrogen	93.27	39.41	126.03	6,65	0
Oxygen	28.31	11.96	85.59	5.61	-50.92
Phospho-lipid	0	0	0.48	0	-0.48
Potass. Sulfate	0	19,309.17	551.72	18,755.89	1.56
Proteins	0	0	0.95	0	-0.95
salt	0	0	0.02	0.83	-0.85
TAG	0	0	4.53	0	-4.53
Water	0	23,782.84	564.15	23,202.89	15.81
TOTAL	121.59	81,893.40	2,520.49	79,495.63	1.14

ratio all have an impact on separation performance (Zhang et al. 2023). Adjusting the operational flow rate in inertial microfluidic separators can significantly affect their ability to separate particles, emphasizing the importance of flow rate control in achieving separation results (Xiang et al. 2019). However, it was stated in the literature that the dimensions and flow rates of spiral microchannels need to be adjusted to achieve a high separation performance (Al-Faqheri et al. 2017; Syed et al. 2018).

This reveals an increase in particle focusing and an improvement in the separation performance of flow rates between 500 and 1500 µL min^{-1} (between 18.3 and 219.4 Reynolds numbers) which is attributed to the strong secondary flow induced at these velocities, leading to a large efficient concentration of cells guided by the Dean Drag force. At the flow rate of 250 µL min^{-1} the microalgae were dominated by Dean Drag force, which were insufficient to concentrate the cells efficiently, and resulting in an inability to collect the microalgae in a concentrated form from the respective outlet channel. Besides, at flow rates of 2000 µL min^{-1} and above, a decrease in the focusing performance was observed which phenomenon is attributed to the intense interaction between particles when a stronger drag force is applied in a small region, and the disruption of stable focusing patterns (Zhao et al. 2017; Lee et al. 2019). Since each microorganism is of different sizes, in order to improve the separation performance, it is important to find the flow rate value that maximizes the efficiency while minimizing stress on the cells and maintaining optimum cell focusing (Bayareh 2020; Choe et al. 2021). Similar to our study, Zhao et al.(2017) used serpentine microchannels and particles of sizes of 3.2 µm, 4.8 µm, 9.9 µm, and 13 µm, and the focusing performance was high between 400 and 1200 µL min^{-1} flow rates.

Studies on the separation of microalgae using microfluidic systems are summarized in Table 5. Upon reviewing the research on the separation of microalgae using microfluidic systems, it could be seen that Syed et al. (2018) successfully separated two different microalgae and achieved the highest performance at the flow rate 1000 µL min^{-1}, with an approximate fractionation efficiency of 80% and a purification efficiency of 95%. Also, Wu et al. (2023) used spiral microchannels to separate microalgae with sizes of 5 µm and 15 µm of the Reynolds number of 66.7, and their purification efficiency was 100%. In another study with spiral microchannels, the separation efficiencies were about 80% for *Chlorella vulgaris* and 72% for *Cosmarium* at a flow rate of 10 µL h^{-1} (Lee & Yao 2018). There are many parameters that affect the separation performance, such as microfluidic type, microfluidic design parameters, microchannel geometry, fluid type, particle number/concentration, as well as the flow rate. For example, in the literature, various methods have been employed for separating bacteria and microalgae, including viscoelastic microfluidics with straight microchannels and removal ratios of over 92% (Yuan et al. 2019), inertial microfluidics with straight microchannels (Godino et al. 2015), and nanosieve devices (Korensky et al. 2021).

In this study we utilized inertial microfluidics with spiral microchannels, which do not require external equipment or chemical additives. The separation performance can be further enhanced by reducing the microalgae concentration, modifying microchannel geometry parameters or the number of turns, and employing two-stage cascaded system in the microfluidic platform. For example, in a study with straight microchannels (Godino et al. 2015), it was proven that separation efficiency, purity, and focusing efficiency decreased with increasing initial concentrations of larger particles. Furthermore, microalgae can be of different sizes, large and small, depending on their stage of cell division and they are commonly regarded as prone to collapse microorganisms (Barros et al. 2019). Over time, microalgae present in the sterile syringe used for inlet flow may precipitate and accumulate within the microchannel flow, potentially affecting experimental results. Additionally, due to the rapid division of bacteria, the possibility of their multiplication between the separation and the subsequent counting of bacteria may also influence the results of the experiment (Scott & Hwa 2011).

Microfluidic devices are highly effective for separating microalgae, but some limitations sould be removed to

Table 5 Various microfluidic devices to separate microalgae

Microalgae Strain	Microfluidic Device	Flow Rates/Reynolds Numbers	References
Chlorella vulgaris & *Haematococcus pluvialis*	PDMS-based 5-turns spiral microchannels	Re = 66.7 (400 µL min^{-1})	(Wu et al. 2023)
Chlorella vulgaris	Asymmetric contraction expansion microchannels to separate microalgae from *Bacillus subtilis* bacteria	Re = 1–15	(Karimi & Sattari-Najafabadi 2023)
Tetraselmis suecica	PDMS-based 5-turns spiral microchannels to separate different sized microalgae	3000 µL min^{-1}	(Magalhães et al. 2023)
Scenedesmus dimorphus	Algae flocculation and coagulation in PDMS-based spiral microchannels	8000 µL min^{-1}	(Sharma & Kim 2022)
Tetraselmis suecica & *Phaeodactylum tricornutum*	PDMS-based 6-turns spiral microchannels	1000 µL min^{-1}	(Mihandoust et al. 2020)
Euglena gracilis	PDMS-based flat microchannel	Re = 77	(Li et al. 2017)
Tetraselmis suecica & *Phaeodactylum tricornutum*	PDMS-based microfluidic device production by soft lithography, spiral microchannels, eight circular loops	1000 µL min^{-1}	(Syed et al. 2018)
Euglena gracilis	PDMS-based microfluidic device, separation of microalgae cells by size difference with hydrogel droplets	Re = 55.7 (500 µL min^{-1})	(Li et al. 2018)
Chlamydomonas reinhardtii	Nanosieve device to separate microalgae cells from *E. coli* bacteria	4–8 µL min^{-1}	(Korensky et al. 2021)
Coenochloris signiensis	PMMA-based microfluidic chip with disposable plastic to separate microalgae cells from *E. coli* bacteria	500 µL min^{-1}	(Godino et al. 2015)
Chlorella vulgaris & *Haematococcus pluvialis*	PDMS-based contraction–expansion array microchannel	Re = 9	(Kim et al. 2021)

achieve optimal efficiency (Abt et al. 2020). High concentrations of microalgae or other particles can cause clogging in the microchannels or fouling, hindering continuous operation and reducing separation efficiency (Ngum et al. 2024). It is essential to consider the design and production stages of the microchannels as they require precise control, and any variation in fabrication can lead to inconsistent performance due to dimensional differences in the channels (Bagi et al. 2024). Furthermore, designs should be modeled using the analyses in large-scale studies to account for the scaling effect. Lastly, achieving high separation efficiency for species with similar properties could be challenging, but active appraoches in hybrid microfluidic systems can assist in obtaining more precise separation (Ebrahimi et al. 2024).

Effects of the microfluidic separation on microalgae cells

The observation of microalgae cells showing a better growth curve after passing through the chip compared to the control group is an important finding. Microalgae cells can be small in size during the stage of new division, but their sizes increase during the growth phases. Additionally, cell sizes can vary depending on culture conditions and the phases from which microalgae are taken from the stock culture. Therefore, the cell size distributions of microalgae in a culture may differ, reported to be between 2–8 µm for *C. minutissima* (Bhatnagar et al. 2010; Stirk et al. 2014). Although this condition may reduce the efficiency of the microfluidic platform, it may have led to the separation of mature cells in the recultivation studies of microalgae and shortened the adaptation time of these microalgae to the fresh medium, resulting in a faster growth curve. Similarly to our study, it has been reported that *C. vulgaris* and *Haematococcus pluvialis* microalgae showed good growth without damage to the cells after being separated using a microfluidic chip and re-cultured (Wu et al. 2023). Korensky et al. (2021) showed that using nanosieve devices, microalgae can be effectively separated from bacteria, and contaminants can be minimized. This could selectively enrich for a more robust or faster-growing microalgae species within the population and may shed light on the reason for the faster growth

of recultivated microalgae. The reasons behind this could be attributed to the cellular mechanisms of stress protection responses such as mannitol production (Rathod et al. 2022), energy storage for endurance (Wang et al. 2022), and metabolic changes triggered by stress conditions, such as the accumulation of triacylglycerides, precursors of lipid accumulation (Hadady et al. 2014). Given these effects and metabolic adaptations, pure microalgae culture may have resulted in a faster growth rate in recultured microalgae compared to the control group.

Carbohydrates and proteins are primary metabolites, while pigments, vitamins, and carotenoids are significant secondary metabolites synthesized by microalgae during culture. Lipids can be categorized as primary or secondary based on their structure and metabolic activities (Vuppaladadiyam et al. 2018). Since the specific growth rate is higher in the post-chip microalgae culture, it is expected that the primary metabolites will increase by 1.5–2 times compared to the untreated microalgae culture. This difference is likely due to the approximately 2.5 times faster growth of post-chip microalgae. However, it is surprising that while the primary metabolites increased, the secondary metabolites also increased. Under stressful conditions such as high salinity, pH, low or high temperature, osmotic stress, microalgae produce much more secondary metabolites such as astaxanthin, β-carotene and render green cells red (Yarkent et al. 2020; Laamanen et al. 2021; Park et al. 2022). In recent years, various microfluidic systems have been designed to induce stress on cells for the purpose of inducing astaxanthin production (Kwak et al. 2015; Cheng et al. 2018; Han, et al. 2019a, b, c; Yao et al. 2020). The simultaneous increase in secondary metabolites while primary metabolites are increasing is likely due to the physical stress microalgae cells undergo when passing through the microfluidic system, such as microchannel geometry and flow rate. In microfluidic systems, hydrodynamic forces such as Dean Drag force and inertial lift force, along with flow rate, can influence the movement and orientation of microalgae, thereby affecting the cell's growth rate, behavior, and shape. Particularly, as the cell diameter increases, the hydrodynamic forces acting on the cell will also increase, which again can induce stress on the cells and may serve as an inducer for secondary metabolites (Krsmanovic et al. 2021; Santore 2022). In addition, the pressure gradient due to secondary flow used for mixing in spiral microchannels (Zhao et al. 2020; Rouhi et al. 2021), the shear stress created by flow velocities on cells (Park et al. 2021), and the injection of cell suspension into the microfluidic system using syringes with small nozzle radii can also induce stress on cells (Guzniczak et al. 2020), triggering cell growth and secondary metabolite production.

Carotene production from green microalgae *Chlorella minutissima*

Chlorella species are a valuable industrial source of many phenolic compounds (Mtaki et al. 2020) and carotenoids, including lutein, α and β-carotene, and astaxanthin (Cha et al. 2008; Ibrahim & Elbialy 2020). Microalgae activate different cellular mechanisms to manage various stress conditions, leading to increased carotenoid production. One of these important mechanisms is the regulation of enzyme expression and the reorganization of metabolic pathways, which entails the downregulation of pathways linked to biomass production and the upregulation of carotenoid biosynthesis pathways (Coesel et al. 2008). Another cellular mechanism is the activation of signaling pathways, which control carotenoid accumulation by triggering stress responses in microalgae (Jo et al. 2020). For example, stress signals caused by nutrient limitation stimulate the expression of genes involved in carotenoid biosynthesis, and carotenoid production increases as a defense mechanism against stressors. In addition, reduced availability of nutrients such as nitrogen can affect the rate of electron transport and the formation of reactive oxygen species in photosystems, which in turn affects carotenoid synthesis (Li et al. 2020). In this respect, there are many studies on increasing the carotene content of microalgae.

Gayathri et al. (2021) optimized aeration and light conditions for lutein production from *Chlorella salina*, Teng et al. (2022) employed aminobutyric acid and pseudo seawater for β-carotene and lutein production from *Chlorella sorokiniana*, Baidya et al. (2021) optimized light conditions for pigment production from *Chlorella ellipsoidea*, Georgiopoulou et al. (2023) studied chlorophyll, carotenoid, and phenolic compound production from *C. vulgaris*, while Morón-Ortiz et al. (2024) optimized extraction methods to enhance carotenoid content from *C. sorokiniana*. Among the *Chlorella* species, *C. minutissima* stands out as a major source of chlorophyll pigments and is also a valuable source of carotenoids, including β-carotene (Sankar et al. 2011; Santos et al. 2023) and phenolics (Selvaraju et al. 2023). The optimization of major and minor nutrients in the medium was reported to trigger carotenoid production (Dineshkumar et al. 2015). For instance, studies on carotenoid production from *C. minutissima* stated that despite being a green microalga species, it could produce carotenoids under extreme conditions, leading to an increase in β-carotene and astaxanthin levels under stress (Ljubic et al. 2021). This is consistent with our results when nutrient stress was applied and concluded as carotene production. Similarly, high nitrogen levels were observed to induce carotene production in *C. minutissima* (Bauer et al. 2020). However, another study found that a decrease in nitrogen levels resulted in

a reduction in carotenoid production (Ördög et al. 2012). In this research, nutrient stress, such as nitrogen, carbon, phosphate, and calcium, was applied to microalgae culture by excluding BG-11 medium ingredients from the media. This manipulation could have induced the microalgae to redirect their metabolic pathways towards carotenoid production. In this study, it was put forth the feasibility effort of a large-scale carotene production -a highly valuable bioactive compound-, from microalgae. *Chlorella minutissima* cells collected after passing through the microfluidic platform can be used in effective carotene production and can be a prominent strategy to increase the sustainability of algal industry. In the literature, there are just a few of research based on large-scale microalgae cultivation for secondary metabolites like carotene. Espada et al. (2020) evaluated β-carotene extraction from *Dunaliella salina* using supercritical CO_2 via SuperPro Designer®. They reported that the potential benefits of the supercritical process in terms of environmental issues do not balance the drawbacks related to its low extraction yield. *D. salina* was grown in open raceways instead of closed photobioreactors due to the economic cost. Chalermthai et al. (2022) studied *D. salina* cultivation, harvesting, and carotene extraction. Similar to Espada et al. (2020), *D. salina* was cultivated in open raceway in that study. It was observed that, both studies disregarded the stress conditions which are the main effect on the induction of carotene production. Other studies such as Razi Parjikolaei et al. (2017) and Monte et al. (2020) investigated only the carotene extraction section of the process. In comparison to those studies, in this study, the aim was to assess all the steps of carotene production from microalgae in this study. Moreover, although fermenter was considered as expensive, fermenters with different scale were preferred due to the control of environmental parameters. This was also included by the study of Marsullo et al. (2015), in achieving high productivity when using closed photobioreactor. It was assumed that the reason for the overestimation could be the temperature control strategy of the reactor, which is kept constant in the simulation runs.

Conclusion

Microalgae are sustainable feedstocks capable of producing primary metabolites under optimal conditions and secondary metabolites such as carotenoids for survival under stress conditions. The cultivation of microalgae in a controlled and reproducible approach is crucial in bioprocesses. Controlled environment of the microalgae cultivation ensures the development of high-quality products and advances economic and environmentally friendly techniques. In this regard, the use of microfluidic devices, which allow fast and high-precision processes by minimizing the amount of waste and chemicals, is limited in microalgal bioprocessing and biotechnology fields. This study employed microfluidic devices with 5-turn spiral microchannels to separate microalgae from bacteria, achieving a success rate of 84.9% separation yield and 93.8% separation purity at a flow rate of 500 mL min^{-1} and a Reynolds number of 36.6. It was demonstrated that post-chip microalgae sustain their viability, showed induced growth and increased the amount of biochemical compounds in comparison with the untreated pure microalgae. Finally, this study demonstrated the industrial feasibility of recultivating post-chip *C. minutissima* for carotenoid production, obtaining a significant increase in carotenoids within 20 days following nutrient stress induction. This study will be critical in terms of the integration of microfluidic systems into microalgae biotechnology, the determination of suitable microchannels and flow rates for separation, the determination of the metabolic effects of microfluidic systems on microalgae cells, and the analysis of the potential for industrial scale carotene production from microalgae. This interdisciplinary research covers innovative technologies in microalgal bioprocesses and carotenoid production from microalgae and will contribute to future research efforts in the field. Near future studies will certainly enhance the effectiveness of separation and purification by using hybrid approaches by also integrating active separation techniques such as dielectrophoresis into the microfluidic system in addition to the passive approach. Moreover, cascade systems, which incorporate many geometries into a single system, could further increase the performance and efficiency.

Acknowledgements The first author was supported by the TUBITAK 2210-A National Scholarship Program for MSc Students. The authors also thank Assoc. Prof. Dr. Azime ERARSLAN for her help in microbiological applications.

Author contribution All authors conceived and designed the experiments. B.K., İ.B., R.M., A.T.K., and B.İ. performed the experiments and all the authors analyzed the data. All authors read and approved the manuscript.

Funding This work was supported by the project no 123M415 of The Scientific and Technological Research Council of Turkey TÜBİTAK 1002-A.

Data availability The authors declare that data supporting the findings of this study are available within the article. Raw data available on request from the authors.

Declarations

Conflict of interest The authors declare no competing interests.

References

Abt V, Gringel F, Han A, Neubauer P, Birkholz M (2020) Separation, characterization, and handling of microalgae by dielectrophoresis. Microorganisms 8:540

Adb el Baky H, El-Baz F, El Baroty G (2008) Evaluation of Marine alga *Ulva lactuca* L. as a source of natural preservative ıngredient. & Environ. Sci 3:434–444

Aghakhani A, Cetin H, Erkoc P, Isik Tombak G, Sitti M (2021) Flexural wave-based soft attractor walls for trapping microparticles and cells. Lab Chip 21:582–596

Ahadian S, Finbloom JA, Mofidfar M, Diltemiz SE, Nasrollahi F, Davoodi E, Hosseini V, Mylonaki I, Sangabathuni S, Montazerian H, Fetah K, Nasiri R, Dokmeci MR, Stevens MM, Desai TA, Khademhosseini A (2020) Micro and nanoscale technologies in oral drug delivery. Adv Drug Deliv Rev 157:37–62

Alam MA, Muhammad G, Rehman A, Russel M, Shah M, Wang Z (2019) Standard techniques and methods for isolating, selecting and monitoring the growth of microalgal strain. In: Alam MA, Wang Z (eds) Microalgae Biotechnology for Development of Biofuel and Wastewater Treatment. Springer, Cham, pp 75–93

Al-Faqheri W, Thio THG, Qasaimeh MA, Dietzel A, Madou M, Al-Halhouli A (2017) Particle/cell separation on microfluidic platforms based on centrifugation effect: A review. Microfluid Nanofluid 21:102

Altay R, Yapici MK, Koşar A (2022) A hybrid spiral microfluidic platform coupled with surface acoustic waves for circulating tumor cell sorting and separation: A numerical study. Biosensors 12:171

Bagi M, Amjad F, Ghoreishian SM, Sohrabi Shahsavari S, Huh YS, Moraveji MK, Shimpalee S (2024) Advances in technical assessment of spiral ınertial microfluidic devices toward bioparticle separation and profiling: A critical review. BioChip J 18:45–67

Baidya A, Akter T, Islam MdR, Shah AKMA, Hossain MdA, Salam MA, Paul SI (2021) Effect of different wavelengths of LED light on the growth, chlorophyll, β-carotene content and proximate composition of *Chlorella ellipsoidea*. Heliyon 7:e08525

Barros A, Pereira H, Campos J, Marques A, Varela J, Silva J (2019) Heterotrophy as a tool to overcome the long and costly autotrophic scale-up process for large scale production of microalgae. Sci Rep 9:13935

Barten R, Chin-On R, De Vree J, Van Beersum E, Wijffels RH, Barbosa MJ, Janssen M (2022) Growth parameter estimation and model simulation for three industrially relevant microalgae: Picochlorum, Nannochloropsis, and Neochloris. Biotechnol Bioeng 119:1416–1425

Bauer LM, Rodrigues E, Rech R (2020) Potential of immobilized *Chlorella minutissima* for the production of biomass, proteins, carotenoids and fatty acids. Biocatal Agric Biotechnol 25:101601

Bayareh M (2020) An updated review on particle separation in passive microfluidic devices. Chemical Engineering and Processing - Process Intensification 153:107984

Bensalem S, Lopes F, Bodénès P, Pareau D, Français O, Le Pioufle B (2018) Understanding the mechanisms of lipid extraction from microalga *Chlamydomonas reinhardtii* after electrical field solicitations and mechanical stress within a microfluidic device. Bioresour Technol 257:129–136

Bhagat AAS, Bow H, Hou HW, Tan SJ, Han J, Lim CT (2010) Microfluidics for cell separation. Med Biol Eng Compu 48:999–1014

Bhagavathy S, Sumathi P, Jancy Sherene Bell I (2011) Green algae *Chlorococcum humicola*-a new source of bioactive compounds with antimicrobial activity. Asian Pac J Trop Biomed 1(Supplement):S1–S7

Bhatnagar A, Bhatnagar M, Chinnasamy S, Das KC (2010) *Chlorella minutissima*—A promising fuel alga for cultivation in municipal wastewaters. Appl Biochem Biotechnol 161:523–536

Bissonnette-Dulude J, Coulombe S, Gervais T, Reuter S (2023) Coupling the COST reference plasma jet to a microfluidic device: A new diagnostic tool for plasma-liquid interactions. Plasma Sources Sci Technol 32:055003

Bligh EG, Dyer WJ (1959) A rapid method of total lipid extraction and purification. Can J Biochem Physiol 37:911–917

Bragheri F, Vázquez RM, Osellame R (2020) Microfluidics. In: Baldacchini T (ed) Three-dimensional microfabrication using two-photon polymerization, 2nd edn. William Andrew Publishing, Oxford, pp 493–526

Cha KH, Koo SY, Lee D-U (2008) Antiproliferative effects of carotenoids extracted from *Chlorella ellipsoidea* and *Chlorella vulgaris* on human colon cancer cells. J Agric Food Chem 56:10521–10526

Chalermthai B, Giwa A, Moheimani N & Taher H (2022) Techno-economic strategies for improving economic viability of β-carotene extraction using natural oil and supercritical solvent: A comparative assessment. Algal Res 68:102875

Cheng X, Qi Z, Burdyny T, Kong T, Sinton D (2018) Low pressure supercritical CO_2 extraction of astaxanthin from *Haematococcus pluvialis* demonstrated on a microfluidic chip. Biores Technol 250:481–485

Choe S, Kim B, Kim M (2021) Progress of microfluidic continuous separation techniques for micro-/nanoscale bioparticles. Biosensors 11:464

Çinar S, Özçimen D, Yılmaz M (2018) Denizel Diatom İzolasyonu, Tanımlanması ve Besin Maddelerinin Diatom Büyümesi Üzerine Etkisinin İncelenmesi. Gazi Üniversitesi Mühendislik-Mimarlık Fakültesi Dergisi 34:1143–1154

Coesel SN, Baumgartner AC, Teles LM, Ramos AA, Henriques NM, Cancela L, Varela JCS (2008) Nutrient limitation is the main regulatory factor for carotenoid accumulation and for *Psy* and *Pds* steady state transcript levels in *Dunaliella salina* (Chlorophyta) exposed to high light and salt stress. Mar Biotech 10:602–611

Dalei J, Sahoo D (2015) Extraction and characterization of astaxanthin from the crustacean shell waste from shrimp processing industries. Int J Pharmaceut Sci Res 6:2532–2537

de Laguna IHB, Marante FJT, Luna-Freire KR, Mioso R (2015) Extraction of nutraceuticals from *Spirulina* (blue-green alga): a bioorganic chemistry practice using thin-layer chromatography. Biochem Mol Biol Educ 43:366–369

Dineshkumar R, Dhanarajan G, Dash SK, Sen R (2015) An advanced hybrid medium optimization strategy for the enhanced productivity of lutein in *Chlorella minutissima*. Algal Res 7:24–32

dos Santos WR, Pereira P, dos Santos LF, Tagliaferro GV (2023) Effects of leachate concentration, carbon dioxide and aeration flow rate on chlorophyll and carotenoid productivity and bioremediation potential of the microalga *Chlorella minutissima*. Water SA 49:387–395

DuBois M, Gilles KA, Hamilton JK, Rebers PA, Smith F (1956) Colorimetric method for determination of sugars and related substances. Anal Chem 28:350–356

Ebrahimi A, Icoz K, Didarian R, Shih CH, Tarim EA, Nasseri B et al (2024) Molecular Separation by using active and passive microfluidic chip designs: a comprehensive review. Adv Mat Interf 11:2300492

Elumalai S, Santhose BI, Kanna GR (2014) Extraction of carotenoid and thin layer chromatography (TLC), GC-MS, FT-IR and HPLC analysis of pharmaceutically important pigment astaxanthin from a new strain of *Haematococcus pluvialis*. Weekly Sci Res J 2:2321–7871

Erdem K, Ahmadi VE, Kosar A, Kuddusi L (2020) Differential sorting of microparticles using spiral microchannels with elliptic configurations. Micromachines 11:412

Espada JJ, Pérez-Antolín D, Vicente G, Bautista LF, Morales V, Rodríguez R (2020) Environmental and techno-economic evaluation of β-carotene production from *Dunaliella salina*. A biorefinery approach. Biofuels Bioprod Bioref 14:43–54

Fernandez-Valenzuela S, Chávez-Ruvalcaba F, Beltran-Rocha JC, San Claudio PM, Reyna-Martínez R (2021) Isolation and

culturing axenic microalgae: mini–review. Open Microbiol J 15:111–119

Gayathri S, Rajasree SRR, Suman TY, Aranganathan L, Thriuganasambandam R, Narendrakumar G (2021) Induction of β,ε-carotene-3,3′-diol (lutein) production in green algae *Chlorella salin*a with airlift photobioreactor: Interaction of different aeration and light-related strategies. Biomass Convers Bioref 11:2003–2012

Georgiopoulou I, Tzima S, Louli V, Magoulas K (2023) Process optimization of microwave-assisted extraction of chlorophyll, carotenoid and phenolic compounds from *Chlorella vulgaris* and comparison with conventional and supercritical fluid extraction. Appl Sci 13:2740

Germond A, Hata H, Fujikawa Y, Nakajima T (2013) The phylogenetic position and phenotypic changes of a *Chlorella*-like alga during 5-year microcosm culture. Eur J Phycol 48:485–496

Godino N, Jorde F, Lawlor D, Jaeger M, Duschl C (2015) Purification of microalgae from bacterial contamination using a disposable inertia-based microfluidic device. J Micromech Microeng 25:084002

Gong Y, Huang J (2020) Characterization of four untapped microalgae for the production of lipids and carotenoids. Algal Res 49:101897

Gou Y, Jia Y, Wang P, Sun C (2018) Progress of ınertial microfluidics in principle and application. Sensors 18:1762

Guzniczak E, Otto O, Whyte G, Willoughby N, Jimenez M, Bridle H (2020) Deformability-induced lift force in spiral microchannels for cell separation. Lab Chip 20:614–625

Hadady H, Wong JJ, Hiibel SR, Redelman D, Geiger EJ (2014) High frequency dielectrophoretic response of microalgae over time. Electrophoresis 35:3533–3540

Han P, Lu Q, Fan L, Zhou W (2019a) A review on the use of microalgae for sustainable aquaculture. Appl Sci 9:2377

Han S-I, Kim HS, Han K-H, Han A (2019b) Digital quantification and selection of high-lipid-producing microalgae through a lateral dielectrophoresis-based microfluidic platform. Lab Chip 19:4128–4138

Han S-I, Yao J, Lee C, Park J, Choi Y-E (2019c) A novel approach to enhance astaxanthin production in *Haematococcus lacustris* using a microstructure-based culture platform. Algal Res 39:101464

Higgins BT, VanderGheynst JS (2014) Effects of *Escherichia coli* on mixotrophic growth of *a minutissima* and production of biofuel precursors. PLoS ONE 9:e96807

Huang D, Man J, Jiang D, Zhao J, Xiang N (2020) Inertial microfluidics: recent advances. Electrophoresıs 41:2166–2187

Huh D, Bahng JH, Ling Y, Wei H-H, Kripfgans OD, Fowlkes JB, Grotberg JB, Takayama S (2007) Gravity-driven microfluidic particle sorting device with hydrodynamic separation amplification. Anal Chem 79:1369–1376

Hyka P, Lickova S, Přibyl P, Melzoch K, Kovar K (2013) Flow cytometry for the development of biotechnological processes with microalgae. Biotechnol Adv 31:2–16

Ibrahim IA, Elbialy ZI (2020) A review: importance of *Chlorella* and different applications. Alexandria J Vet Sci 65:16–34

İnan B, Koçer AT, Özçimen DB (2023) Valorization of lignocellulosic wastes for low-cost and sustainable algal biodiesel production using biochar-based solid acid catalyst. J Anal Appl Pyrol 173:106095

Jalilian MR (2008) Spectra and structure of binary azeotropes: IV. Acetone–cyclohexane. Spectrochim Acta A 69:812–815

Jo SW, Hong JW, Do JM, Na H, Kim JJ, Park SI, Kim YS, Kim IS, Yoon HS (2020) Nitrogen deficiency-dependent abiotic stress enhances carotenoid production in ındigenous green microalga *Scenedesmus rubescens* KNUA042, for use as a potential resource of high value products. Sustainability 12:5445

Joseph S, Ramadoss DM, Chellandi M (2022) Photoinhibition and β-carotene production from *Dunaliella* sp. isolated from salt pans of Goa. Biomass Conv Bioref. https://doi.org/10.1007/s13399-022-03327-x

Karacaoğlu B (2024) Using microfluidic systems for microalgal bioprocess and biotechnology. Master of Science Thesis, Yildiz Technical University, p 90

Karacaoğlu B, Bütün İ, Mercimek R, İnan B, Koşar A, Balkanlı D (2023) Fabrication of a microfluidic platform for the isolation of Polar microalgae from Antarctica. Paper presented at AlgaEurope 2023, Prague, Czech Republic, pp 12–15

Karacaoğlu B, İnan B, Balkanlı Özçimen D (2023b) Microfluidic systems as a novel approach for microalgal bioprocess. Biochem Eng J 197:108959

Karimi A, Sattari-Najafabadi M (2023) Numerical study of bacteria removal from microalgae solution using an asymmetric contraction-expansion microfluidic device: A parametric analysis approach. Heliyon 9:e20380

Kim GY, Son J, Han JI, Park JK (2021) Inertial microfluidics-based separation of microalgae using a contraction–expansion array microchannel. Micromachines 12(1):97

Kim HS, Devarenne TP, Han A (2018) Microfluidic systems for microalgal biotechnology: A review. Algal Res 30:149–161

Koçer AT, İnan B, Kaptan Usul S, Özçimen D, Yılmaz MT & Işıldak İ (2021) Exopolysaccharides from microalgae: production, characterization, optimization and techno-economic assessment. Braz J Microbiol 52(4):1779–1790

Koçer AT, İnan B, Özçimen D, Gökalp İ (2023) A study of microalgae cultivation in hydrothermal carbonization process water: Nutrient recycling, characterization and process design. Environ Technol Innov 30:103048

Koçer AT, Mutlu B, Özçimen D (2020) Investigation of biochar production potential and pyrolysis kinetics characteristics of microalgal biomass. Biomass Convers Biorefin 10:85–94

Kolackova M, Janova A, Dobesova M, Zvalova M, Chaloupsky P, Krystofova O, Adam V, Huska D (2023) Role of secondary metabolites in distressed microalgae. Environ Res 224:115392

Korensky G, Chen X, Bao M, Miller A, Lapizco-Encinas B, Park M, Du K (2021) Single *Chlamydomonas reinhardtii* cell separation from bacterial cells and auto-fluorescence tracking with a nanosieve device. Electrophoresıs 42:95–102

Krsmanovic M, Biswas D, Ali H, Kumar A, Ghosh R, Dickerson AK (2021) Hydrodynamics and surface properties influence biofilm proliferation. Adv Coll Interface Sci 288:102336

Kwak HS, Kim JYH, Sim SJ (2015) A microreactor system for cultivation of *Haematococcus pluvialis* and astaxanthin production. J Nanosci Nanotech 15:1618–1623

Laamanen CA, Desjardins SM, Senhorinho GNA, Scott JA (2021) Harvesting microalgae for health beneficial dietary supplements. Algal Res 54:102189

Lambert JB (1987) Introduction to organic spectroscopy. Macmillan, London

Lee JH, Lee SK, Kim JH, Park JH (2019) Separation of particles with bacterial size range using the control of sheath flow ratio in spiral microfluidic channel. Sens Actuators A 286:211–219

Lee M-L, Yao D-J (2018) The separation of microalgae using Dean flow in a spiral microfluidic device. Inventions 3:40

Lee TH-W, Show P-L, Ong HC, Ling TC, Lan JC-W, Chang J-S (2020) Microalgae ısolation and cultivation technology for mass production. In: Bisaria V (ed) Handbook of Biorefinery Research and Technology. Springer, Dordrecht, pp 1–29

Lin B (ed) (2011) Microfluidics: technologies and applications. Springer, Cham

Li M, Muñoz HE, Goda K, Di Carlo D (2017) Shape-based separation of microalga *Euglena gracilis* using inertial microfluidics. Sci Rep 7:10802

Li M, van Zee M, Goda K, Di Carlo D (2018) Size-based sorting of hydrogel droplets using inertial microfluidics. Lab Chip 18:2575–2582

Lingadahalli Kotreshappa S, Nayak CG, Krishnan Venkata S (2023) A review on the role of microflow parameter measurements for microfluidics applications. Systems 11:113

Li X, Sun H, Mao X, Lao Y, Chen F (2020) Enhanced Photosynthesis of carotenoids in microalgae driven by light-harvesting gold nanoparticles. ACS Sust Chem Eng 8:7600–7608

Ljubic A, Holdt SL, Jakobsen J, Bysted A, Jacobsen C (2021) Fatty acids, carotenoids, and tocopherols from microalgae: Targeting the accumulation by manipulating the light during growth. J Appl Phycol 33:2783–2793

Lowry OH, Rosebrough NJ, Farr AL, Randall RJ (1951) Proteın measurement wıth the Folın phenol reagent. J Biol Chem 193:265–275

Macías-Sánchez MD, Mantell C, Rodríguez M, Martínez de la Ossa E, Lubián LM, Montero O (2005) Supercritical fluid extraction of carotenoids and chlorophyll a from *Nannochloropsis gaditana*. J Food Eng 66:245–251

Magalhães VH, Pinto VC, Sousa PJ, Gonçalves LM, Fernández E, Minas G (2023) A microfluidic device for size-based microplastics and microalgae separation. In: 2023 IEEE 7th Portuguese Meeting on Bioengineering (ENBENG). IEEE, pp 56–59

Maltsev Y, Maltseva K, Kulikovskiy M, Maltseva S (2021) Influence of light conditions on microalgae growth and content of lipids, carotenoids, and fatty acid composition. Biology 10:1060

Mariana G, Corina M, Alina C, Sanda B (2016) Determination of carotenoids by thin layer chromatography. Analele Universităţii din Oradea XXVI:247–252

Marsullo M, Mian A, Ensinas AV, Manente G, Lazzaretto A, Marechal F (2015) Dynamic modeling of the microalgae cultivation phase for energy production in open raceway ponds and flat panel photobioreactors. Front Energy Res 3:41

Martel JM, Toner M (2014) Inertial focusing in microfluidics. Annu Rev Biomed Eng 16:371–396

Mihandoust A, Maleki-Jirsaraei N, Rouhani S, Safi S, Alizadeh M (2020) Improvement of size-based particle separation throughput in slanted spiral microchannel by modifying outlet geometry. Electrophoresıs 41:353–359

Minyuk G, Sidorov R, Solovchenko A (2020) Effect of nitrogen source on the growth, lipid, and valuable carotenoid production in the green microalga *Chromochloris zofingiensis*. J Appl Phycol 32:923–935

Mishra S, Liu Y-J, Chen C-S, Yao D-J (2021) An easily accessible microfluidic chip for high-throughput microalgae screening for biofuel production. Energies 14:1817

Monte J, Ribeiro C, Parreira C, Costa L, Brive L, Casal S, Brazinha C, Crespo JG (2020) Biorefinery of *Dunaliella salina*: Sustainable recovery of carotenoids, polar lipids and glycerol. Biores Technol 297:122509

Morón-Ortiz Á, Mapelli-Brahm P, León-Vaz A, Benitez-González AM, León R, Meléndez-Martínez AJ (2024) Ultrasound-assisted extraction of carotenoids from phytoene-accumulating *Chlorella sorokiniana* microalgae: Effect of milling and performance of the green biosolvents 2-methyltetrahydrofuran and ethyl lactate. Food Chem 434:137437

Mtaki K, Kyewalyanga MS, Mtolera MSP (2020) Assessment of antioxidant contents and free radical-scavenging capacity of *Chlorella vulgaris* cultivated in low cost media. Appl Sci 10:8611

Mu X, Zheng W, Sun J, Zhang W, Jiang X (2013) Microfluidics for manipulating cells. Small 9:9–21

Neha T, Shishir T, Ashutosh D (2017) Fourier transform infrared spectroscopy (FTIR) profiling of red pigment produced by *Bacillus subtilis* PD5. Afr J Biotech 16:1507–1512

Ngum LF, Matsushita Y, El-Mashtoly SF, Fath El-Bab AMR, Abdel-Mawgood AL (2024) Separation of microalgae from bacterial contaminants using spiral microchannel in the presence of a chemoattractant. Bioresour Bioprocess 11:36

Onyeaka H, Miri T, Obileke K, Hart A, Anumudu C, Al-Sharify ZT (2021) Minimizing carbon footprint via microalgae as a biological capture. Carbon Capt Sci Technol 1:100007

Ördög V, Stirk WA, Bálint P, van Staden J, Lovász C (2012) Changes in lipid, protein and pigment concentrations in nitrogen-stressed *Chlorella minutissima* cultures. J Appl Phycol 24:907–914

Otzen DE, Buell AK, Jensen H (2021) Microfluidics and the quantification of biomolecular interactions. Curr Opin Struct Biol 70:8–15

Özbey A, Karimzadehkhouei M, Kocatürk NM, Erbil Bilir S, Kutlu Ö, Gözüaçık D, Koşar A (2019) Inertial focusing of cancer cell lines in curvilinear microchannels. Micro Nano Eng 2:53–63

Ozdalgic B, Ustun M, Dabbagh SR, Haznedaroglu BZ, Kiraz A, Tasoglu S (2021) Microfluidics for microalgal biotechnology. Biotechnol Bioeng 118:1716–1734

Paparella A, Shaltiel-Harpaza L, Ibdah M (2021) β-Ionone: Its Occurrence and biological function and metabolic engineering. Plants 10:754

Park C, Bae J, Choi Y, Park W (2021) Shear stress-triggered deformation of microparticles in a tapered microchannel. Polymers 13:55

Park YH, Han S-I, Oh B, Kim HS, Jeon MS, Kim S, Choi Y-E (2022) Microalgal secondary metabolite productions as a component of biorefinery: a review. Bioresour Technol 344:126206

Pérez JP, Muñoz AA, Figueroa CP, Agurto-Muñoz C (2021) Current analytical techniques for the characterization of lipophilic bioactive compounds from microalgae extracts. Biomass Bioenerg 149:106078

Quijano-Ortega N, Fuenmayor CA, Zuluaga-Dominguez C, Diaz-Moreno C, Ortiz-Grisales S, García-Mahecha M, Grassi S (2020) FTIR-ATR spectroscopy combined with multivariate regression modeling as a preliminary approach for carotenoids determination in *Cucurbita* spp. Appl Sci 10:3722

Rajput A, Singh DP, Khattar JS, Swatch GK, Singh Y (2022) Evaluation of growth and carotenoid production by a green microalga *Scenedesmus quadricauda* PUMCC 4.1.40. Under optimized culture conditions. J Basic Microbiol 62:1156–1166

Ratha SK, Rao PH, Govindaswamy K, Jaswin RS, Lakshmidevi R, Bhaskar S, Chinnasamy S (2016) A rapid and reliable method for estimating microalgal biomass using a moisture analyser. J Appl Phycol 28:1725–1734

Rathod JP, Vira C, Lali AM, Prakash G (2022) Heterologous mannitol-1-phosphate dehydrogenase gene over-expression in *Parachlorella kessleri* for enhanced microalgal biomass productivity. J Genetic Eng Biotech 20:38

Razi Parjikolaei B, Errico M, El-Houri RB, Serrano CM, Fretté X, Christensen KV (2017) Process design and economic evaluation of green extraction methods for recovery of astaxanthin from shrimp waste. Chem Eng Res Des 117:73–82

Rouhi O, Razavi Bazaz S, Niazmand H, Mirakhorli F, Mas-hafi S, Amiri H, Miansari M, Ebrahimi Warkiani M (2021) Numerical and experimental study of cross-sectional effects on the mixing performance of the spiral microfluidics. Micromachines 12:1470

Rusdianasari R, Hakim L, Kalsum L (2021) The optimum yield of *Nannochloropsis* sp microalgae from the lipid cultivation and extraction process with Soxhlet method. Indones J Fundament Appl Chem 6:81–89

Sankar V, Daniel DK, Krastanov A (2011) Carbon dioxide fixation by *Chlorella minutissima* batch cultures in a stirred tank bioreactor. Biotechnol Biotechnol Equip 25:2468–2476

Santore MM (2022) Interplay of physico-chemical and mechanical bacteria-surface interactions with transport processes controls early biofilm growth: A review. Adv Coll Interface Sci 304:102665
Scott M, Hwa T (2011) Bacterial growth laws and their applications. Curr Opin Biotechnol 22:559–565
Selvaraju K, Raguraman V, Yadav HN, Hariprasad P, Malik A (2023) Spectral characterization and binding dynamics of bioactive compounds from *Chlorella minutissima* against α-glucosidase: An in vitro and in silico approach. Algal Res 75:103281
Sharma R, Kim M (2022) Enhanced microalgae harvesting in a microfluidic centrifugal separator. Biomass Bioenerg 159:106386
Singh N, Batghare AH, Choudhury BJ, Goyal A, Moholkar VS (2020) Microalgae based biorefinery: assessment of wild fresh water microalgal isolate for simultaneous biodiesel and β-carotene production. Bioresour Technol Rep 11:100440
Singh P, Gupta SK, Guldhe A, Rawat I, Bux F (2015) Microalgae isolation and basic culturing techniques. In: Kim SK (ed) Handbook of Marine Microalgae. Academic Press, NY, pp 43–54
Sousa V, Pereira RN, Vicente AA, Dias O, Geada P (2023) Microalgae biomass as an alternative source of biocompounds: New insights and future perspectives of extraction methodologies. Food Res Int 173:113282
Stirk WA, Bálint P, Tarkowská D, Novák O, Maróti G, Ljung K, Turečková V, Strnad M, Ördög V, van Staden J (2014) Effect of light on growth and endogenous hormones in *Chlorella minutissima* (Trebouxiophyceae). Plant Physiol Biochem 79:66–76
Syed MS, Rafeie M, Vandamme D, Asadnia M, Henderson R, Taylor RA, Warkiani ME (2018) Selective separation of microalgae cells using inertial microfluidics. Bioresour Technol 252:91–99
Takeungwongtrakul S, Benjakul S, Santoso J, Trilaksani W, Nurilmala M (2015) Extraction and stability of carotenoid-containing lipids from hepatopancreas of Pacific white shrimp (*Litopenaeus vannamei*). J Food Process Preserv 39:10–18
Teng C-S, Xue C, Lin J-Y, Ng I-S (2022) Towards high-level protein, beta-carotene, and lutein production from *Chlorella sorokiniana* using aminobutyric acid and pseudo seawater. Biochem Eng J 184:108473
Tong CY, Honda K, Derek CJC (2023) A review on microalgal-bacterial co-culture: The multifaceted role of beneficial bacteria towards enhancement of microalgal metabolite production. Environ Res 228:115872
Vanapalli SA, Duits MHG, Mugele F (2009) Microfluidics as a functional tool for cell mechanics. Biomicrofluidics 3:012006
Veltri LM, Holland LA (2020) Microfluidics for personalized reactions to demonstrate stoichiometry. J Chem Educ 97:1035–1040
Vu CHT, Lee H-G, Chang YK, Oh H-M (2018) Axenic cultures for microalgal biotechnology: Establishment, assessment, maintenance, and applications. Biotechnol Adv 36:380–396
Vuppaladadiyam AK, Prinsen P, Raheem A, Luque R, Zhao M (2018) Microalgae cultivation and metabolites production: a comprehensive review. Biofuels Bioprod Biorefin 12:304–324
Wang C, Qi M, Guo J, Zhou C, Yan X, Ruan R, Cheng P (2022) The active phytohormone in microalgae: the characteristics, efficient detection, and their adversity resistance applications. Molecules 27:46
Wang Y, Wang J, Cheng J, Zhang Y, Ding G, Wang X, Chen M, Kang Y, Pan X (2020) Serial separation of microalgae in a microfluidic chip under ınertial and dielectrophoretic forces. IEEE Sens J 20:14607–14616
Woggon W-D (2002) Oxidative cleavage of carotenoids catalyzed by enzyme models and beta-carotene 15,15´-monooxygenase. Pure Appl Chem 74:1397–1408
Wu Z, Zhao M, Liu Z, Shi L, Li T, Zhou T (2023) Microalgae separation using spiral inertial microchannel. Microfluid Nanofluid 27:23
Xiang N, Wang J, Li Q, Han Y, Huang D, Ni Z (2019) Precise size-based cell separation via the coupling of ınertial microfluidics and deterministic lateral displacement. Anal Chem 91:10328–10334
Yan S, Zhang J, Yuan D, Li W (2017) Hybrid microfluidics combined with active and passive approaches for continuous cell separation. Electrophoresıs 38:238–249
Yang Y, Chen Y, Tang H, Zong N, Jiang X (2020) Microfluidics for biomedical analysis. Small Methods 4:1900451
Yao J, Kim HS, Kim JY, Choi YE, Park J (2020) Mechanical stress induced astaxanthin accumulation of *H. pluvialis* on a chip. Lab on a Chip 20:647–654
Yarkent Ç, Gürlek C, Oncel SS (2020) Potential of microalgal compounds in trending natural cosmetics: a review. Sustainable Chem Pharm 17:100304
Yuan D, Zhao Q, Yan S, Tang S-Y, Zhang Y, Yun G, Nguyen N-T, Zhang J, Li M, Li W (2019) Sheathless separation of microalgae from bacteria using a simple straight channel based on viscoelastic microfluidics. Lab on a Chip 19:2811–2821
Zaid RM, Chong FC, Teo EYL, Ng E-P, Chong KF (2015) Reduction of graphene oxide nanosheets by natural beta carotene and its potential use as supercapacitor electrode. Arab J Chem 8:560–569
Zhang T, Inglis DW, Ngo L, Wang Y, Hosokawa Y, Yalikun Y, Li M (2023) Inertial separation of particles assisted by symmetrical sheath flows in a straight microchannel. Anal Chem 95:11132–11140
Zhao Q, Yuan D, Yan S, Zhang J, Du H, Alici G, Li W (2017) Flow rate-insensitive microparticle separation and filtration using a microchannel with arc-shaped groove arrays. Microfluid Nanofluid 21:55
Zhao Q, Yuan D, Zhang J, Li W (2020) A review of secondary flow in ınertial microfluidics. Micromachines 11:461
Zou N, Richmond A (2000) Light-path length and population density in photoacclimation of *Nannochloropsis* sp. (Eustigmatophyceae). J Appl Phycol 12:349–354